Environment International 192 (2024) 109018

Contents lists available at ScienceDirect

Environment International

journal homepage: www.elsevier.com/locate/envint

Full length article

Transcriptomic and functional effects from a chemical mixture based on the exposure profile in Baltic Sea salmon, on metabolic and immune functions in zebrafish embryo

Carolina Vogs [a,b,1], Dennis Lindqvist [a,c,1], Sheung Wai Tang [a], Lydia Gugescu [a], Harri Alenius [a,d], Emma Wincent [a,*]

[a] Unit of System Toxicology, Institute of Environmental Medicine, Karolinska Institutet, Box 210, SE 171 77, Stockholm, Sweden
[b] Division of Pharmacology and Toxicology, Department of Animal Biosciences, Swedish University of Agricultural Sciences, Box 7023, SE 750 07, Uppsala, Sweden
[c] Department of Environmental Science, Stockholm University, SE 106 91, Stockholm, Sweden
[d] Human Microbiome Research, Faculty of Medicine, University of Helsinki, Box 63, 00014 Helsinki, Finland

ARTICLE INFO

Handling Editor: Adrian Covaci

Keywords:
Baltic Sea mixture toxicity
Halogenated toxins
Immunotoxicity
Metabolic disruption

ABSTRACT

The Baltic Sea is one of the world's most contaminated seas with long-standing adverse health status of its wildlife such as the Baltic Sea salmon, resulting in reduced fecundity and increased mortality. While adverse health effects have been reported among wild fish from the Baltic Sea, the toxicity mechanisms underlying these adversities, and the chemical effect drivers mediating them are poorly understood. To address this knowledge gap, we utilized the zebrafish (*Danio rerio*) embryo model to determine molecular and functional effects brought on by exposure to a technical mixture including 9 organohalogen compounds detected in serum from wild-caught Baltic Sea salmon. To align with the salmon exposure scenario, an internal dose regimen was opted to establish same relative proportions of the compounds in the zebrafish (whole body) as observed in the salmon serum. Through transcriptomic profiling, we identified dose-dependent effects on immune system and metabolism as two critical functions overlapping with adverse effects observed in wild fish from the Baltic Sea. We then determined likely effect drivers by comparing gene responses of the mixture with those of individual mixture components. Aligned with our transcriptome results, the number of total macrophages was reduced and the zebrafish's ability to respond to a tissue damage suppressed in a dose-dependent manner. This study brings forth a key advancement in delineating the impact of chemical pollutants on the health of wild fish in the Baltic Sea.

1. Introduction

The adverse health status of wildlife in the Baltic Sea has been an issue for decades, alongside its extensive chemical pollution. This is evident in several animal species, including the Baltic Sea salmon (*Salmo salar*), which during the last 8 years have displayed reduced fecundity and increased mortality. Although the severity of the salmon health status has varied over the years, they show a wide range of symptoms culminating in an inability or apathy towards traversing the rivers to the spawning grounds (Weichert, 2021). This has been associated to severe fungal infections and skin lacerations, in many cases with a lethal outcome (Brockmark, 2017; Brockmark, 2019), with viral and bacterial infections proposed as the most plausible causes of the observed skin conditions (SVA, 2017). While these studies suggest an impaired immune system as a contributing factor, very few studies have been conducted to elucidate the underlying mechanisms and the possible role of chemical pollutants in the increase in infections and declining health.

The Baltic Sea is one of the most contaminated seas in the world and is heavily polluted with numerous types of compounds. Although the chemical landscape has changed over the last decades, the major contaminants belong to the group of organohalogens, including per- and polyfluorinated (PFAS), brominated, and chlorinated compounds, many of which are inherently persistent and thereby accumulate in the Baltic Sea biota. Most of these compounds stem from anthropogenic sources.

* Corresponding author.
E-mail addresses: carolina.vogs@slu.se (C. Vogs), dennis.lindqvist@ki.se (D. Lindqvist), lidia.gugescu@ki.se (L. Gugescu), harri.alenius@ki.se (H. Alenius), emma.wincent@ki.se (E. Wincent).
[1] Shared first author.

https://doi.org/10.1016/j.envint.2024.109018
Received 1 July 2024; Received in revised form 12 September 2024; Accepted 16 September 2024
Available online 24 September 2024

However, some are also formed by natural processes, e.g., by filamentous algae (Löfstrand, 2011; Malmvärn et al., 2008), which may be potentiated by an increased coverage of the algae caused by nutrient enrichment (Bonsdorff et al., 2002; Helcom, 2009), or by an increased production due to external stressors such as elevated temperature (Dahlgren et al., 2015).

Levels of several PFAS, including perfluorooctanesulfonic acid (PFOS) and perfluorooctanoic acid (PFOA), have been observed to increase over the last 30–40 years in the liver of Baltic Sea herring (Faxneld, 2016; Miller, 2014). The same is true for hydroxylated polybrominated diphenyl ethers (OH-PBDEs) (Faxneld et al., 2014), of which 6-OH-BDE47 is the dominant congener measured in fish (Dahlgren et al., 2016), seals (Lindqvist et al., 2017), and marine birds (Dahlgren et al., 2016). In a recent study, we identified 41 organohalogen compounds in serum of Baltic Sea salmon collected 2018 during spawning migration at the river Umeälven connected to the Baltic Sea in the north of Sweden (Lindqvist and Wincent, 2022). Based on their relative prevalence in the serum and prior knowledge regarding toxicity, 9 of these were selected and evaluated for their toxicokinetic and toxicity parameters in zebrafish (*Danio rerio*) embryos, individually as well as in a technical mixture, using the same relative internal doses among the compounds in zebrafish (whole body) as detected in the salmon serum (Lindqvist and Wincent, 2022). Several dose-dependent morphological effects were observed, including scoliosis, edemas, reduced growth, and abolished swim-bladder inflation. While the individual components of the mixture caused different effect-profiles, most morphological effects appeared in an additive manner when exposed as a mixture.

As morphological and phenotypic alterations alone are insufficient to reveal toxicant-induced effect mechanisms, more detailed knowledge about underlying molecular mechanisms of adverse health effects is needed. In this study, we performed advanced transcriptomic profiling and gene-network analysis of zebrafish embryo exposed to the technical mixture, and compared the major effects observed between exposure to the mixture with that of individual compounds. Our aims were to identify affected biological functions and pathways that may reveal the underlying toxicity mechanisms, to identify the mixture components driving these effects, and to determine the functional consequences of this. By implementing an exposure regimen based on internal dose profiles rather than external (nominal) dose, thereby omitting toxicokinetic differences of the chemicals between fish species, this study brings forth a key advancement in delineating the impact of chemical pollutants and their adverse effect mechanisms on wild fish in the Baltic Sea.

2. Materials and methods

2.1. Determination of chemical mixtures and doses

Based on chemical analysis of serum from Baltic Sea salmon, a technical mixture consisting of 9 out of 41 detected halogenated compounds was established depending on their levels in the salmon serum and/or available data on toxicity (Lindqvist and Wincent, 2022).

The 9 compounds included were dichlorodiphenyldichloroethylene (DDE; a degradation product of the pesticide DDT), pentachlorophenol (PCP; a chlorinated pesticide), PCB118 (a polychlorinated biphenyl (PCB)), 4-OH-CB187 (a hydroxylated PCB), 6-OH-BDE47, 6-OH-BDE90 and 2′-OH-BDE68 (hydroxylated polybrominated diphenyl ethers; OH-PBDEs), PFOS and PFOA (perfluorinated persistent organic pollutants). The rational underlying the selection of these compounds was previously described in detail (Lindqvist and Wincent, 2022). Briefly, the pesticides DDE and PCP were included due to the high concentration of DDE in the salmon serum and high potency of PCP to disrupt mitochondrial function. PCB118 was selected as a representative PCB and 4-OH-CB187 was included due to being the most abundance OH-PCB. 6-OH-BDE90 was included as the most abundant OH-PBDE congener, 2′-OH-BDE68 as the most frequently monitored congener, and 6-OH-BDE47 as the most toxic congener acting as protonophoric uncoupler as well as an inhibitor of complex II of the electron transport chain. PFOS and PFOA represented a perfluorinated sulfonic acid and perfluorinated carboxylic acid, respectively, of which PFOS was the compound with highest concentration of all in the salmon serum.

As these compounds do not occur at equal magnitudes in nature, and their uptake may differ between type of compound and fish species, our aim was to maintain their relative proportions as observed in the salmon serum to assess the effect of a relevant chemical composition instead of assessing the compounds effects in a one-to-one relationship. Thus, a technical mixture was created in order to establish a similar relative magnitude between respective compound in the zebrafish embryo tissue at day 5 post fertilization (dpf), and their relative magnitude observed in salmon serum. The tuning of external doses to reach the desired internal doses, by chemical analysis of exposure media and whole-body embryos at different times and doses, was extensively described in our previous work (Lindqvist and Wincent, 2022). Throughout the study, two sub-toxic doses of the mixture were used based on previous toxicity testing (Lindqvist and Wincent, 2022), with dose 1 and dose 2 corresponding to 0.3 and 0.6 times the dose causing morphological effects (not including non-inflated swim bladder) in 10 % (EC10) of the embryos. Nominal (external) doses and internal doses in zebrafish embryo estimated at respective dose at 3- and 5 days exposure are presented in Table 1. Note that the bioconcentration of PFOS and PFOA is strongly dose dependent

Table 1
Nominal external doses, internal doses, and area under the curves (AUC) determined at 1-, 3-, and 5-days (D) of exposure. External doses ([Nom]) are stated for individual compounds included in the mixture dose 1 and dose 2 (nM), as well as the total dose of the mixture including all compounds (μM). The external dose of the technical mixture was established to reach the relative internal dose level of each compound at 5 days post fertilization in the zebrafish as measured in serum of wild Baltic Sea salmon (Lindqvist and Wincent, 2022).

	External dose	Internal dose μM			μMD	μMD
Dose 2	**[Nom] nM**	**[Zf] D1**	**[Zf] D3**	**[Zf] D5**	**AUC D3**	**AUC D5**
DDE	48.1	23.2	32.4	38.0	67.3	137.7
PCB118	3.2	1.58	2.74	3.90	5.10	11.74
PCP	0.3	0.21	0.39	0.37	0.70	1.47
4-OH-CB187	0.3	0.60	0.30	0.29	1.20	1.78
6-OH-BDE47	24.4	9.75	3.82	2.02	18.45	24.30
2′-OH-BDE68	5.7	5.10	1.34	1.23	8.98	11.56
6-OH-BDE90	101	14.0	3.8	2.6	24.8	31.1
PFOS	3001	71.8	224	358	332	913
PFOA	700	1.28	3.78	6.42	5.71	15.91
Total (μM)	***3.89***					
	External dose	**Internal dose μM**			**μMD**	**μMD**
Dose 1	**[Nom] nM**	**[Zf] D1**	**[Zf] D3**	**[Zf] D5**	**AUC D3**	**AUC D5**
DDE	24.0	11.6	16.2	19.0	33.6	68.9
PCB118	1.61	0.79	1.37	1.95	2.55	5.87
PCP	0.13	0.10	0.20	0.19	0.35	0.73
4-OH-CB187	0.16	0.30	0.15	0.14	0.60	0.89
6-OH-BDE47	12.2	4.88	1.91	1.01	9.23	12.1
2′-OH-BDE68	2.84	2.55	0.67	0.62	4.49	5.78
6-OH-BDE90	50.7	7.00	1.89	1.30	12.4	15.6
PFOS	1501	41.1	131	204	193	528
PFOA	350	0.90	2.56	4.51	3.91	11.0
Total (μM)	***1.94***					

†[Nom]: nominal external dose, [Zf]: internal dose, μMD: total internal dose (AUC) at 1, 3 or 5 days (D) exposure.

and hence a 2-fold increase in external dose does not cause a 2-fold increase in internal dose, as discussed in previous work (Lindqvist and Wincent, 2022; Tal and Vogs, 2021). For investigating functional effects, additional doses were included as indicated in the results section.

2.2. Zebrafish husbandry, exposure, and sampling

Zebrafish at 0-5dpf were used throughout the study, including wildtype strain (AB) and strains reporting the expression of neutrophils (*Tg(LysC:dsRED)*) or macrophages (*Tg(mpeg1:gal4-UAS:NTR-mCherry)*). Embryos were provided by the Zebrafish Core facility at Comparative Medicine, Karolinska Institutet, approximately 2 h post fertilization (hpf), and were exposed at 3 hpf in glass petri-dishes, with 30 embryos per dish in 30 mL of embryo medium (E3; 5.0 mM NaCl, 0.17 mM KCl, 0.33 mM $CaCl_2$, 0.33 mM $MgSO_4$, 2 mM HEPES, pH 7). DMSO (0.01 %) was used as vehicle control in all studies, and exposures never exceeded 0.01 % DMSO. Exposures were initiated by adding the compound(s) to the E3 directly, followed by thorough mixing. Toxicity was monitored daily, and dead embryos were removed continuously. For RNA sequencing and RT-qPCR analysis, ten pooled embryos were sampled in sets of 5 or 3 biological replicates, respectively, at both 3- and 5 dpf. Afterwards, sampled embryos were stored at 4 °C in RNAprotect (Qiagen, Hilden, Germany) until RNA extraction was performed using the RNeasy Plus universal mini kit (Qiagen, Hilden, Germany). The concentration of respective sample was determined using Nanodrop One (Thermo Fisher Scientific, MA, USA), and RNA integrity was determined using an Agilent 2100 Bioanalyzer (Agilent Technologies, CA, USA) prior to further analysis.

2.3. RNA sequencing

Total RNA was subjected to quality control with Tapestation (Agilent Technologies, CA, USA) according to the manufacturer's instructions. To construct libraries suitable for Illumina sequencing, the Illumina Trueseq stranded mRNA protocol was used, including mRNA isolation, cDNA synthesis, ligation of anchors and amplification and indexing of the libraries. The yield and quality of the amplified libraries were analyzed using Qubit (Thermo Fisher Scientific) and Tapestation (Agilent Technologies). The indexed cDNA libraries were normalized using Qubit and combined and the pools were sequenced on the Illumina Nextseq 550 on a High Output v2.5 flowcell, generating 75 bp single-end reads.

Raw read counts for a total of 32,520 genes were obtained, which, after removing those with a raw read count lower than 10, resulted in 26,504 remaining genes (81 % of total counts). Ensembles were annotated with terms corresponding to zebrafish (ZFIN) and human (HGNC) orthologue symbols using R package biomaRt (version 2.50.0). Normalization of raw read counts was conducted using DESeq2 (version 1.34.0), and principal component analysis (PCA) was performed to assess the quality of the expression matrix. Log2fold changes (Log2FC) and p-values (Wald test) were calculated for the two mixture doses compared to the vehicle controls at 3 and 5dpf, respectively. The p-values were adjusted for multiple hypothesis testing using the Benjamin-Hochberg (B-H) procedure. Differentially expressed genes (DEGs) were defined as genes that had an absolute Log2FC value $\geq$ 0.38 (corresponding to a fold change of 1.3) and a B-H adjusted p-value $\leq$ 0.05. An upset diagram was plotted using UpSetR (version 1.4.0) to summarize the number of HGNC-annotated DEGs across different exposures.

2.4. Pathway analysis

HGNC-annotated DEGs were used for analysing biological pathways and functions, as required by thedownstream analysis tools used in this study. Reactome pathway analysis at hierarchy level three was performed with R shiny application FunMappOne (Scala et al., 2019). For the identification of enriched Reactome pathway terms, a minimum of three genes per pathway and a "g:SCS" adjusted p-value $\leq$ 0.05 were set as thresholds. Jaccard index with complete linkage was selected for similarity clustering. The amplitude of gene fold changes was summarized for each enriched functional term by the aggregation function "mean". Enriched term lists with adjusted p-values were exported and the figure appearance was finalized in Excel (Microsoft Windows 10, version 2301).

As described in Marwah *et al.* 2018 (Marwah, 2018), Inference of Network Response Modules (INfORM) was applied to generate co-expression networks and to identify gene modules for the HGNC-annotated DEGs. A gene co-expression network was derived by combining multiple networks inferred from the gene expression profiles. The gene networks were generated by using different network inference algorithms (ARACNE, MRNET, CLR, and mutual information-based methods). The compiled networks were then merged to define an ensemble gene network that included only high-confidence edges. Gene modules were identified in the network by using the community detection algorithm Walktrap and evaluated based on multiple metrics of node importance. Next, we wanted to identify the molecular and cellular functions affected by the mixture exposure based on the INfORM-determined clusters of DEGs. Therefore, clusters of DEGs associated with the gene modules at 3 and 5dpf, respectively, were analyzed using the Ingenuity Pathway Analysis software (IPA; Qiagen, version 84978992) to identify molecular and cellular functions significantly affected, and the predicted activation or suppression of these. Inclusion criteria for categories of functions were set at B-H adjusted p-value $\leq$ 0.05 and predicted activity (z-score) $\geq$ 1.5 for functions annotations included in these categories.

2.5. Identification of effect drivers

We further aimed to identify chemical effect drivers in the observed transcriptomic changes, potentially caused by one or multiple individual compounds in the mixture. To this end, genes with an absolute log2FC $\geq$ 0.68 (3dpf) or $\geq$ 0.85 (5dpf) were selected from respective INfORM gene module. By multiplying the log2FC of respective gene with its B-H adjusted p-value ($-\log(padj)$), ranking scores were produced incorporating both quantitative and qualitative parameters. Based on the calculations, 6–17 genes per gene module were identified as having scores $\geq$ 5 together with being annotated to the predominant functional processes identified in the IPA analysis. Expression of these genes was thereafter analyzed in zebrafish embryos either exposed to the chemical mixture or selected individual mixture components at 3 and 5 dpf, respectively. As this assessment included extensive exposure analysis, we selected five of the nine compounds to investigate further (i.e., 6-OH-BDE47, 6-OH-BDE90, PCP, DDE, and PFOS) based on their abundance in the salmon serum together with our previous toxicity data (Lindqvist and Wincent, 2022). Exposures to the individual compounds and mixture doses were conducted as described before.

2.6. RT-qPCR analysis

An aliquot corresponding to 1 μg of total RNA from respective RNA extract was transcribed to cDNA using the iScript kit (Bio-Rad Laboratories, CA, USA) and a Bio-Rad MyCycler thermocycler, following the protocol provided with the kit. RT-qPCR analyses were thereafter performed using gene specific primers or probes, as presented in Table 1 in the supplement. The PCR reaction mixes were prepared using the PowerSYBR Green PCR Master Mix and TaqMan Gene Expression Assays (Applied Biosystems), for primers and probes respectively, following the protocol of the supplier. The PCRs were conducted on a QuantStudio 5 Real-Time PCR system (Applied Biosystems). Protocols for the PCR are found in Table 2 in the supplement. Relative gene expression levels were calculated using the ddCT equation. Genes that were expressed below detection level or that displayed non-specific or aberrant amplification plots were discarded from further analysis. Euclidean distance analysis (Tyanova, 2016) was thereafter used to identify hierarchical clustering

between the expression of gene-sets selected from each module. Statistical significance between expression of gene-sets induced by chemical mixtures or single compounds exposure was determined using Pearson correlation (GraphPad Prism version 9.0.0 for Mac OS X, GraphPad Software, San Diego, California USA).

2.7. Immune cell development and function

Recruitment of immune cells to a tissue damage was determined as means to assess the functional consequences of the exposures, using copper sulphate (Cu) induced damage of hair cells in the neuromasts of the lateral line according to previously published procedures (d'Alencon, 2010). Similar to the previous exposure regimen, embryos from the *Tg(LysC:dsRED)* (neutrophils) and *Tg(mpeg1:mCherry)* (macrophages) strains were exposed at 3hpf to the mixture and individual mixture components, separately, as well as to negative control (no Cu), vehicle control (DMSO; 0.01 %) and positive control (Indomethacin; 30 μM). Doses were selected to include a wider range compared to the transcriptomics analysis, starting at Dose 1 as lowest dose, and up to 3.5 times that dose (EC10; 6.8 μM). Exposures to the individual mixture components corresponded to their respective dose at the highest mixture dose. At 3dpf, the embryos were treated with copper sulfate in two separate concentrations (10 and 30 μM). Any unhatched embryos were mechanically removed from the chorion prior to treatment, and embryos with visible defects were excluded. At two hours (neutrophil reporter) or three hours (macrophage reporter) post-treatment the embryos were transferred to a new petri-dish and sedated using Tricaine (0.036 mg/mL), followed by imaging using a Nikon SMZ25 (Nikon corporation, Tokyo, Japan) with an excitation range from 528 to 553 nm and emission range from 590 to 650 nm. Images were processed using the ImageJ (1.52 h) software (National Institute of Health, MD, USA). The lateral line was selected, and the images were converted to black and white after which immune cell recruitment was measured as the relative area of fluorescent cells within the lateral line. Outliers having values more than 1.5 times the interquartile range below or above the 1st and 3d quartile, respectively, were removed. Normality was tested using the Kolmogorov-Smirnov test, and Kruskal Wallis was performed to determine significant differences in cell recruitment relative to the DMSO control (Cu treated), using Dunn's test to correct for multiple comparisons.

Effects on the total number of live macrophages (without tissue damage) were determined by flow cytometry analysis of pooled embryo homogenates (n = 25 embryos per sample). At 3dpf the exposed embryos *Tg(mpeg1:mCherry)* were anesthetized on ice until all visible movements ceased. All water was removed and 300 μl dissociation mix was added per sample (0.05 % trypsin-EDTA, 20 mg/ml collagenase (Merck)) and incubated at 32 °C, followed by pipetting until no visible tissue was left. The homogenates were transferred to ice and 1 ml DMEM without phenol red supplemented with 5 % FBS (ThermoFischer) was added to respective sample before centrifugation at 300G for 10 min at 4 °C. The cells were thereafter separated from the remaining debris by filtering the suspension through a 40 um mesh then resuspended in DMEM with 5 % FBS and kept on ice until analysis. To assess cell viability, the cells were stained with 1 ug/ml DAPI (BD bioscience) 5–10 min prior to analysis. Samples were acquired on a LSR Fortessa instrument (BD bioscience). DAPI was excited by a 405 nm laser at 100 mW with a detection filter at 450/50 nm and mCherry was excited by a 561 nm laser at 100 mW with a detection filter at 610/20 nm. Single color controls were analyzed to confirm that spectral compensation was unnecessary; the mCherry positive gate was set using mCherry coated compensation beads (BrightComp eBeads™ Compensation Bead Kits, ThermoFischer). The samples were analysed using FlowJo software (version 10.9.0). Two-sided *t*-test was performed to determine significant differences in number of live macrophages per sample relative to the DMSO control.

3. Results

3.1. Dose- and time-dependent transcriptional responses of mixture exposure

Comparing DEG coverage using zebrafish (ZFIN) and human (HGNC) orthologues showed 75–95 % overlap depending on dose and duration of exposure (Table 3 in supplement). All downstream analyses were performed using the HGNC annotated dataset as required for these analyses. As seen in the UpSet diagram in Fig. 1A, 5dpf generated 296 and 362 DEGs in total at dose 1 and dose 2, respectively, of which 69 overlapped between the doses. Much fewer DEGs were observed at 3dpf, totaling 53 and 102 genes at dose 1 and dose 2, respectively, with an overlap of 21 DEGs. Only five genes were found to be significantly affected in all exposure conditions, namely the protein coding genes *prss57, pon2, cyp3a7, socs3 and dhrs13*. Hence, time appears to be the bigger factor compared to dose causing an increased number of DEGs. This observation is underlined by the PCA analysis that attributed 81 % of the variance in the transcriptome to exposure time as illustrated in supplementary fig. 1. However, when stratified to 3 and 5dpf, 57 % and 82 % of the variance in the first two PCA dimensions resulted from dose effects, respectively.

In addition to time- and dose-dependent differences in number of DEGs, distinct functional effects were identified within the Reactome pathway analysis, with 5dpf showing more significantly affected biological pathways than 3dpf (Fig. 1B). At 3dpf, an aggregated mean of an increased fold-change in all genes related to metabolism, biotransformation, and response to reactive oxygen species (ROS) was observed, mainly at dose 2. Increased expression of metabolism-associated genes was observed also at 5dpf, in a dose-dependent manner. In contrast, dose 1 showed a clear suppression in genes related to immune system signaling and functions associated with both innate and adaptive immunity and cytokine signaling. Additional biological processes suppressed at 5dpf related to for example cell death, cell cycle, DNA replication, and DNA synthesis. The DEGs included in respective process is shown in supplementary Table 4, together with information on the number of DEGs in the dataset mapped to respective process and the gene ratio.

Next, gene network analysis was performed to identify clusters of co-expressed DEGs at 3 and 5dpe, respectively, across both doses (Fig. 2). In total, three and four gene clusters of co-expressed DEGs, from here on referred to as gene modules 1 to 7, were identified at 3 and 5dpf, respectively. The complete list of DEGs clustered in the seven modules is provided in supplementary Table 5. At 3dpf, the three gene modules included 30 (e.g. *ctrl, ctrb2, pmp2, dpep1*), 36 (e.g., *cyp1a1, gstp1, gsr, cyp3a4*), and 47 (e.g., fabp6, slc14a2, abcb11, fkbp5) DEGs, respectively (Fig. 2A). Module 1 mainly consisted of DEGs from dose 1, while DEGs from dose 2 dominated modules 2 and 3. Similar trends were seen at 5dpf (Fig. 2B), where the four distinct modules included 199 (e.g., *mx1, irf1, ehf, casp1*), 214 (e.g., *fosb, slc14a2, cidec, cyp24a2*), 103 (e.g., *elovl2, ugdh, fads2, abcb11*), and 24 (e.g., *slc26a2, creb3l3, ugt2a3, pklr*) DEGs, respectively. In these, DEGs in dose 1 dominated module 4, while DEGs in dose 2 dominated modules 5 and 7, and module 6 contained a similar number of DEGs in both doses (63 vs. 84).

To delineate biological significances of the identified gene modules, we next performed Ingenuity Pathway 'core analyses' of respective module, assessing the categories of affected molecular and cellular functions, the functional annotations within these categories, and their predicted directions of effect. At 3dpf, the significantly affected molecular and cellular categories in module 1 related mainly to protein homeostasis, cellular growth and function, and, to a lesser extent, metabolism (supplementary Fig. 2A). The functional annotations did, however, not display any statistically significant direction of effects (z-score). Module 2 displayed dose-dependent effects predominantly on metabolism of e.g., drugs, lipids, vitamins and minerals, carbohydrates, and others, in addition to effects on molecular transport, radical

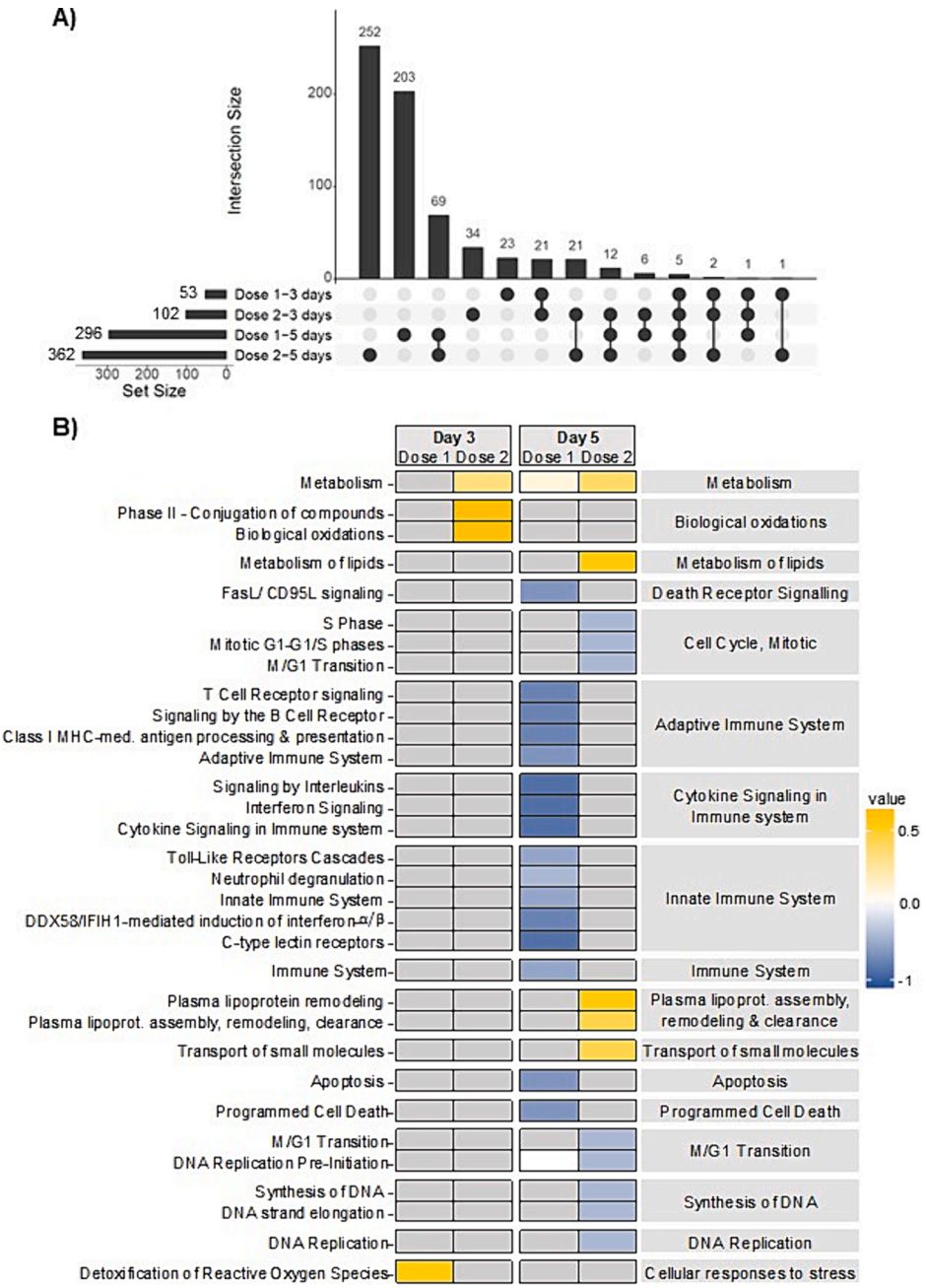

Fig. 1. Dose- and developmental stage dependent effects on biological processes. A) UpSet diagram of differently expressed genes, defined by cut-off of log2 foldchange (LOG2FC) 0.38 and adjusted p-value 0.05. B) REACTOME pathway of biological processes associated with exposure to chemical mixture dose 1 and dose 2, at day 3 and 5 post fertilization. Minimum of three genes per pathway were clustered by similarity (jaccard, complete linkage) and by different study groups at the 3rd REACTOME level, $p < 0.05$. Yellow color indicates a positive aggregated mean of the LOG2FC, and blue represents a negative aggregated mean of the LOG2FC, with the intensity of color representing level of LOG2FC value. (For interpretation of the references to color in this figure legend, the reader is referred to the web version of this article.)

scavenging, gene expression and cellular homeostasis (Fig. 3A). These function categories were further defined by functional annotations indicating increased cell viability, increased quantity of carbohydrates and conversion of lipids, as well as suppressed cell movement, and reduced levels of ROS and inflammation. In module 3, only dose 2 showed significant effects on molecular and cellular functions (Fig. 3B). Aside from this difference, the functional annotations showed partial overlap with module 2 regarding effects on metabolism, cell homeostasis and function, quantity of ROS, and inflammation.

At 5dpf, a more distinct difference in functional and dose-dependent effects was observed compared to 3dpf, and with higher statistical significance. In module 4, mainly dose 1 contained annotations pointing to significant suppression of immune system development and function (Fig. 4A), while modules 5 and 6 mainly contained effects on metabolism and cell viability, mediated by dose 2, or both doses, respectively (Fig. 4B and supplementary Fig. 2B). Altogether, these data suggest the metabolic and immune systems as critical targets for the mixture of organohalogen compounds, and further pointed to differences in time- and dose-dependence for the observed effects.

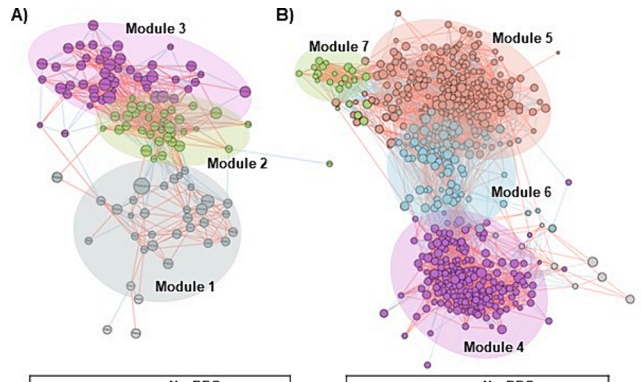

3dpf	Nr. DEGs		
	Module	Dose 1	Dose 2
Module 1	30	30	13
Module 2	36	14	35
Module 3	47	0	47

5dpf	Nr. DEGs		
	Module	Dose 1	Dose 2
Module 4	199	197	22
Module 5	214	15	214
Module 6	103	63	84
Module 7	24	0	24

Fig. 2. Co-expressed gene networks and modules. Network analysis of co-expressed genes associated with different doses (dose 1 and dose 2) at A) 3 days post fertilization (dpf), and B) 5dpf. Associated tables state the total number of differentially expressed genes (DEGs) at respective gene module, and dose. Modules are highlighted with shaded areas.

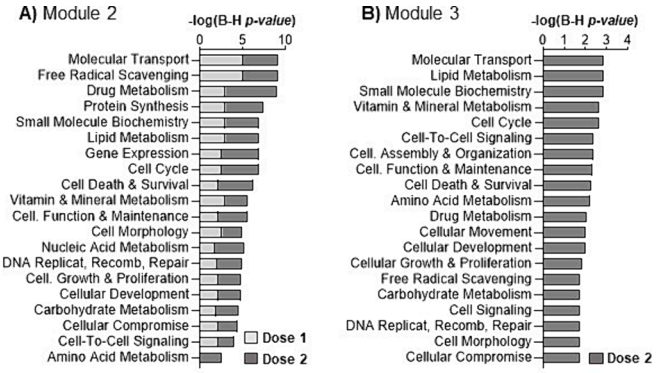

Dose 1: Functions Annotation	B-H p-value	z-score
Cell viability	1.3×10^{-2}	1.6
Apoptosis	1.1×10^{-2}	-1.9
Cell movement	4.6×10^{-2}	-1.8
Leukocyte migration	2.3×10^{-2}	-1.7
Quantity of ROS	3.4×10^{-06}	-1.6
Dose 2: Functions Annotation		
Cell survival	7.6×10^{-3}	2.7
Cell viability	1.2×10^{-2}	2.5
Quantity of adipose tissue	1.6×10^{-2}	2.0
Concentration of D-glucose	2.6×10^{-2}	1.9
Quantity of carbohydrate	2.8×10^{-2}	1.8
Conversion of lipid	1.4×10^{-4}	1.7
Inflammation of body cavity	1.9×10^{-3}	-2.2

Dose 2: Functions Annotation	B-H p-value	z-score
Cell survival	7.6×10^{-2}	2.6
Cell viability	1.2×10^{-2}	2.5
Cell death of epithelial cells	1.2×10^{-2}	2.4
Apoptosis of epithelial cells	1.2×10^{-2}	2.2
Export of molecule	1.2×10^{-3}	2.0
Ion homeostasis of cells	1.6×10^{-2}	2.0
Quantity of metal	2.6×10^{-2}	1.7
Transport of molecule	2.8×10^{-3}	1.6
Synthesis of lipid	1.4×10^{-3}	1.5
Inflammation of organ	1.5×10^{-2}	-2.5
Cell. infiltration by lymphocytes	9.7×10^{-3}	-2.0
Generation of ROS	2.0×10^{-2}	-1.9
Inflammation of body cavity	1.7×10^{-2}	-1.8

Fig. 3. Molecular and cellular functions significantly affected at 3 days post fertilization (dpf). Bar graphs show stacked –log BH adjusted p-values for the top 20 categories of significantly affected molecular and cellular functions of Dose 1 and Dose 2 in A) Module 2, and B) Module 3, with –log BH adjusted p-values below 1.3 ($p < 0.05$.

3.2. Drivers of mixture effects

To better understand the individual contribution of the mixture components on the observed effects, we next exposed zebrafish embryos to five compounds representative of the mixture (6-OH-BDE47, 6-OH-BDE90, PCP, DDE and PFOS), separately, at concentrations corresponding to their levels in dose 1 (LOW) and dose 2 (HIGH) of the mixture (Table 1). At 3 and 5dpf, relative gene expression derived from respective gene module were determined, focusing on functional annotations related to drug metabolism (3dpf, module 2), metabolic

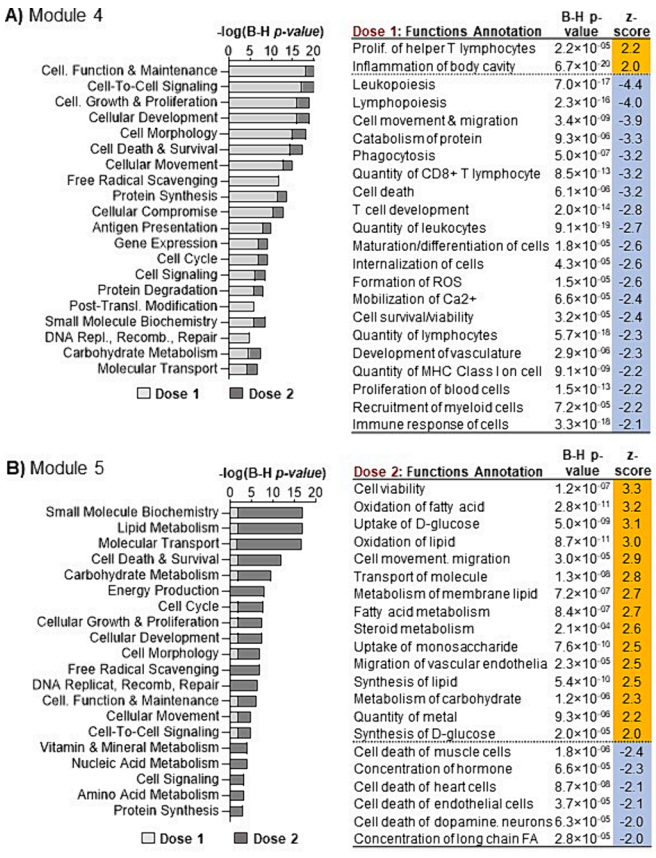

Dose 1: Functions Annotation	B-H p-value	z-score
Prolif. of helper T lymphocytes	2.2×10^{-05}	2.2
Inflammation of body cavity	6.7×10^{-20}	2.0
Leukopoiesis	7.0×10^{-17}	-4.4
Lymphopoiesis	2.3×10^{-16}	-4.0
Cell movement & migration	3.4×10^{-09}	-3.9
Catabolism of protein	9.3×10^{-06}	-3.3
Phagocytosis	5.0×10^{-07}	-3.2
Quantity of CD8+ T lymphocyte	8.5×10^{-13}	-3.2
Cell death	6.1×10^{-06}	-3.2
T cell development	2.0×10^{-14}	-2.8
Quantity of leukocytes	9.1×10^{-19}	-2.7
Maturation/differentiation of cells	1.8×10^{-05}	-2.6
Internalization of cells	4.3×10^{-05}	-2.6
Formation of ROS	1.5×10^{-05}	-2.6
Mobilization of Ca2+	6.6×10^{-05}	-2.4
Cell survival/viability	3.2×10^{-05}	-2.4
Quantity of lymphocytes	5.7×10^{-18}	-2.3
Development of vasculature	2.9×10^{-06}	-2.3
Quantity of MHC Class I on cell	9.1×10^{-09}	-2.2
Proliferation of blood cells	1.5×10^{-13}	-2.2
Recruitment of myeloid cells	7.2×10^{-05}	-2.2
Immune response of cells	3.3×10^{-16}	-2.1

Dose 2: Functions Annotation	B-H p-value	z-score
Cell viability	1.2×10^{-07}	3.3
Oxidation of fatty acid	2.8×10^{-11}	3.2
Uptake of D-glucose	5.0×10^{-09}	3.1
Oxidation of lipid	8.7×10^{-11}	3.0
Cell movement, migration	3.0×10^{-05}	2.9
Transport of molecule	1.3×10^{-06}	2.8
Metabolism of membrane lipid	7.2×10^{-07}	2.7
Fatty acid metabolism	8.4×10^{-07}	2.7
Steroid metabolism	2.1×10^{-04}	2.6
Uptake of monosaccharide	7.6×10^{-10}	2.5
Migration of vascular endothelia	2.3×10^{-05}	2.5
Synthesis of lipid	5.4×10^{-10}	2.5
Metabolism of carbohydrate	1.2×10^{-06}	2.3
Quantity of metal	9.3×10^{-06}	2.2
Synthesis of D-glucose	2.0×10^{-05}	2.0
Cell death of muscle cells	1.8×10^{-06}	-2.4
Concentration of hormone	6.6×10^{-05}	-2.3
Cell death of heart cells	8.7×10^{-08}	-2.1
Cell death of endothelial cells	3.7×10^{-05}	-2.1
Cell death of dopamine. neurons	6.3×10^{-05}	-2.0
Concentration of long chain FA	2.8×10^{-05}	-2.0

Fig. 4. Molecular and cellular functions significantly affected at 5 days post fertilization (dpf). Bar graphs show stacked –log BH adjusted p-values for the top 20 categories of significantly affected molecular and cellular functions of Dose 1 and Dose 2 in A) Module 4, and B) Module 5, with –log BH adjusted p-values below 1.3 (p-value) < 0.05.

homeostasis (3dpf, module 3; 5dpf, modules 5–6), and immune system function (5dpf, module 4). Cellular and molecular functions from respective gene modules with an absolute z-score of ≥ 1.5 were selected (Figs. 3-4), and ranking scores of genes within each function were calculated, resulting in a list of genes from respective day, dose, and module (supplementary Table 6). As shown in Fig. 5 and supplementary Table 7, some functional effects were predominantly associated to one compound, while others seemed to be affected by several of the included compounds. For example, at 3dpf, effects on drug metabolizing enzymes and antioxidant enzymes such as *cyp1a, cyp3a7, gsr, gstp1 and prdx1* (module 2) appeared to be driven mainly by 6-OH-BDE90 (90LOW and 90HIGH), while the other compounds demonstrate either weak associations or partially opposite trends compared to the mixture, especially for expression of gluthathion reductase (*gsr*) and *cyp1a* (Fig. 5A). In contrast, all compounds except DDE displayed statistically significant correlations to the mixture effect on genes associated with metabolic homeostasis in module 3 (supplementary Table 7, Fig. 5B). Notably, only 6-OH-BDE47 (47LOW and 47HIGH) showed a strong suppression of the gene *fabp6* (fatty acid binding protein 6), similar to the mixture exposure, indicating a compound-specific effect on fatty acid transport. At 5dpf, a combination of positive and negative associations between individual compounds and mixture effects on immune system function was observed in module 4 (supplementary Table 7, Fig. 5C). Here, different degrees of overlap were seen across the gene set and between doses, with 6-OH-BDE90 showing the strongest overlap with the mixture, and PCP demonstrating a clear induction of all but one gene (*mx; myxovirus (influenza) resistance A*), as opposed to the overall suppression observed with the mixture. The genes affected most similarly across exposures were *mx, dram 1, stat4* and *s100a1*, while *psmb8a ehf,*

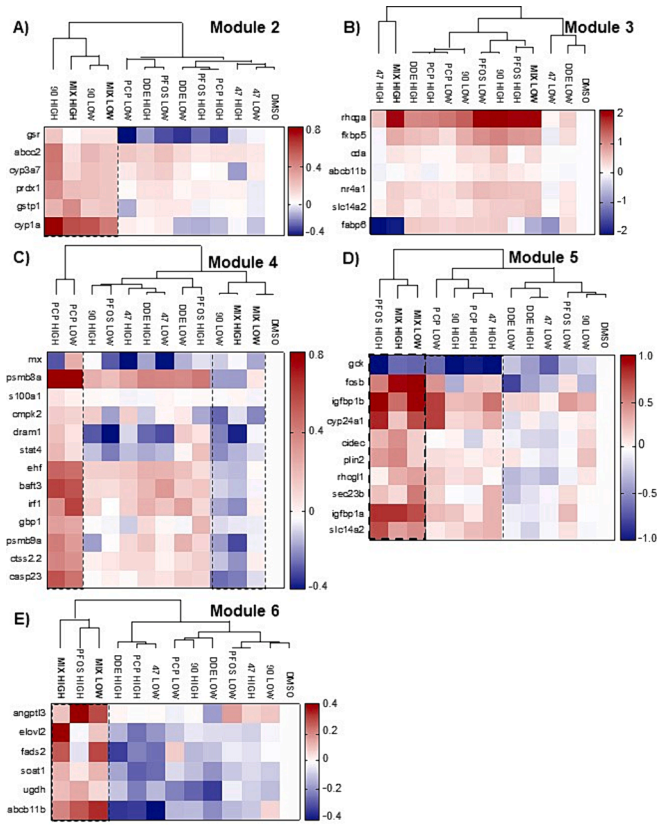

Fig. 5. Drivers of mixture effects at 3- and 5- days post fertilization (dpf). Euclidian cluster analysis of gene expression associated to functional processes at 3dpf in A) module 2, and B) module 3, as well as at 5dpf in C) module 4, D) module 5, and E) module 6, at exposure to the mixture and separate mixture components. LOW and HIGH refers to dose 1 and dose 2, respectively. Each value represents the average log2 fold-change of triplicate samples, and dashed lines highlights exposures correlating or contradicting with the mixture.

baft3, and i*rf1* showed a uniform opposite effect with all individual compounds but 6-OH-BDE90, compared to the mixture. Similar to 3dpf, all compounds but DDE showed statistically significant effects on genes related to metabolic homeostasis in module 5 (supplementary Table 7, Fig. 5D), such as *gck, igfbp1b, cyp24a1* and *plin 2*. In contrast, only PFOS (dose 2) showed significant correlation with the mixture effect on metabolic effects in module 6 (supplementary Table 7, Fig. 5E), including genes such as *angptl3, elovl2, soat1, ugdh* and *abcb11b*. Overall, these results point to a mix of compound- and dose-dependent impact on some effects, while other effects may require a mixture of two or more compounds to cause the observed effects.

3.3. *Effects on immune function*

Considering the significant suppression of immune system development and function observed at the transcriptional level (module 4), we next performed a tissue injury model to determine effects on immune cell recruitment to a tissue damage. Here, we used Cu (10 μM) to cause inflammation in the zebrafish embryos by damaging the hair cells in the lateral line of the 3dpf embryos (d'Alencon, 2010). Upon hair cell damage, neutrophils and macrophages translocate to the lateral line to assist in the hair cell damage response and repair, leading to an accumulation of these cells in the lateral line (figure 6A). As seen in figure 6B, a dose-dependent suppression of neutrophil recruitment to the lateral line was observed by the mixture exposure compared to vehicle control (DMSO). Moreover, four of the nine individual mixture components caused a significant suppression (6-OH-BDE47, 6-OH-BDE90, 2′-OH-BDE68, 4-OH-CB187), while the remaining five did not (PFOS, PFOA, DDE, PCP, PCB118). Similar effects were seen with macrophage recruitment to the lateral line (data not shown), with the significant difference that an apparent reduction in total number of macrophages was observed (supplementary Fig. 4), interfering with the readout. To study this further, the total number of live macrophages was determined after exposure to the mixture and mixture components without concomitant injury, showing a significant dose-dependent reduction of macrophages by the mixture (Fig. 6C). Importantly, 6-OH-BDE47 appears to be the dominant compound mediating this effect, as it was the only individual compound causing a significant reduction of macrophages.

4. Discussion

The Baltic Sea has been heavily polluted throughout history. Due to the limited water exchange through the Danish straits, the turn-over time over the water mass is long, leading to accumulation of numerous anthropogenic chemicals. Several chemical classes of concern have been detected in Baltic Sea wildlife including potentially harmful pesticides, PCBs, PFAS, and naturally produced algal toxins (Dahlgren, et al., 2022; Bjurlid et al., 2018; Airaksinen, 2014; Lindqvist, 2020; de Wit, 2020). While adverse effects on reproductive and immune system functions have been reported for Baltic Sea fish, other wildlife species, and animals fed contaminated fish from the Baltic Sea (Dahlgren, et al., 2022; Bergman, 1999; Nyman et al., 2002; Sonne, 2020; Förlin, 2019); the underlying toxicity mechanisms and chemical effect drivers caused by mixture exposures are poorly understood.

In this study, we investigated transcriptional profiles in zebrafish embryo exposed to a technical mixture consisting of 9 anthropogenic chemicals and natural algal toxins detected in serum of Baltic Sea salmon. Using the same mixture composition and dosing strategy, we previously showed that the naturally produced algal toxin 6-OH-BDE47 dominantly contributed to severe morphological effects observed in zebrafish embryo, even though the internal concentration of 6-OH-BDE47 was orders of magnitude lower than the anthropogenic chemicals DDE, PCB118, PFOS and PFOA (Lindqvist and Wincent, 2022). It must be noted, however, that the body burden of chemicals in wildlife fish undergo seasonal trends, for instance shown for naturally produced brominated chemicals that peaked in perch sampled from the Baltic Sea over the summer months (Dahlgren et al., 2016; Gustafsson, 2021). Furthermore, concentrations of anthropogenic chemicals in Baltic Sea wild fish vary between sampling locations and over time for many regulated chemicals such as PCBs and PFAS (Bignert et al., 2016). Therefore, the molecular and functional effects identified here in zebrafish embryo represent only a snapshot of mixture exposure faced by Baltic Sea salmons at the time and place of sampling. Nonetheless, our study stands in stark contrast to previous experimental studies that explored the consequences of Baltic Sea exposures, as they included only anthropogenic chemicals or natural algal toxins, separately, not taking into account the presence of co-exposure to both sources (Halden, 2011; Kammann, 2004; Legradi, 2014), along with performing solely targeted effect analysis. In addition to experimental studies, several ecoepidemiology studies have been performed in which chemical exposures measured in different Baltic Sea wildlife species were associated with biochemical effect biomarkers such as concentration of glucose and plasma lactate, ethoxyresorufin-O-deethylase (EROD) activity, oxidative stress status in addition to morphometric indices (Dahlgren, et al., 2022; Förlin, 2019; Gustafsson, 2021). However, those studies did not account for mixture effect associations, impairing the identification of mixture toxicity drivers and their potential interactions. Moreover, the impact of chemcial mixtures mimicking real-life Baltic Sea exposure on global transcriptional changes in wild fish has been reported previously only in two studies, using livers of perch and salmon, respectively (Förlin, 2019; Kanerva et al., 2020). While the aims of these studies were associated to changes in effects over time, fish origin and habitat environment, they also revealed exposure-associated effects on biological processes such as

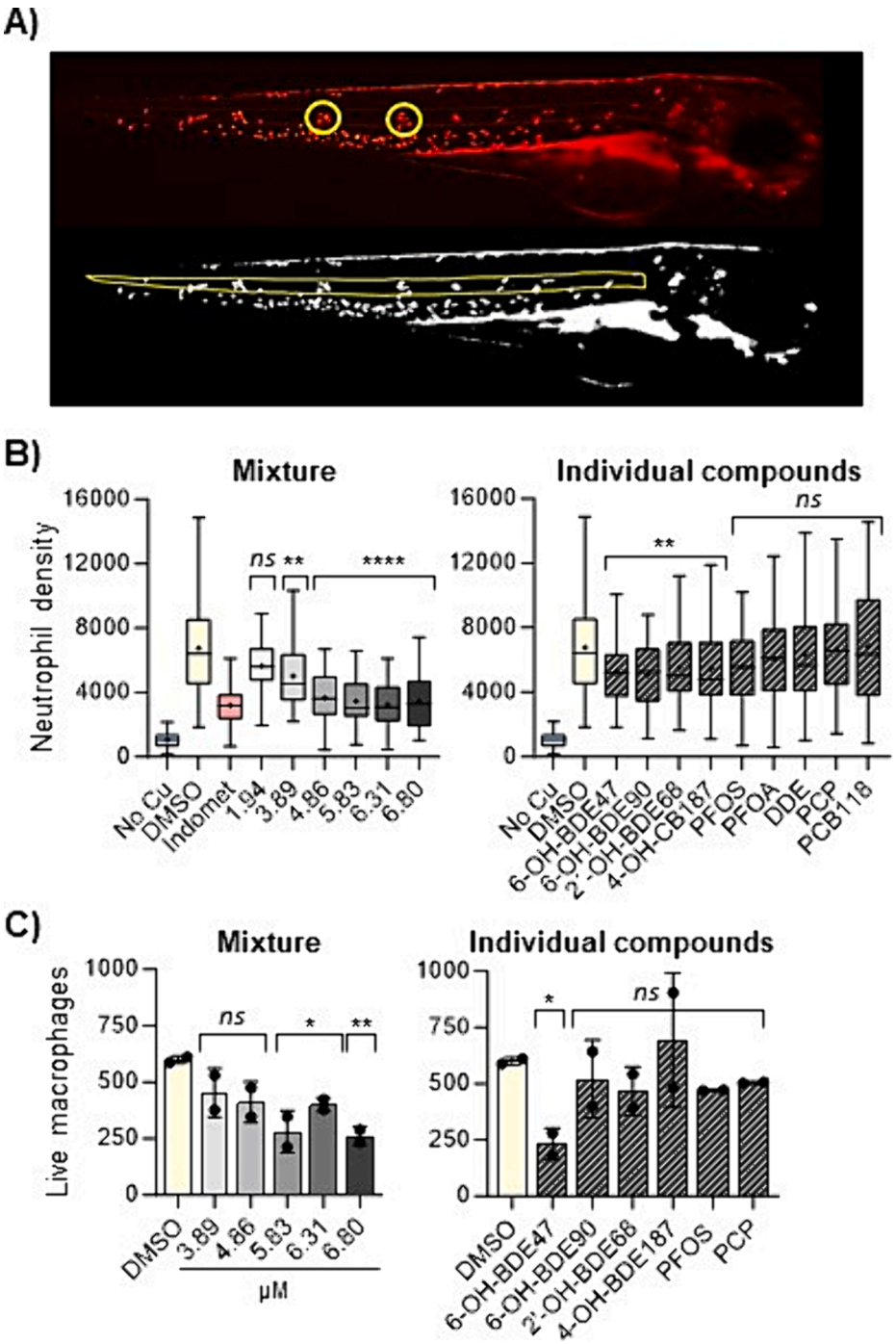

Fig. 6. Effects on immune function. A) images illustrating the neutrophil accumulation at the damaged hair cells in the lateral line, indicated by the circles. B) Neutrophil density at the lateral line without damage (no Cu, neg control) and after Cu-induced damage in embryos pre-exposed to vehicle control (DMSO), positive control (Indomethacin), a dose-range of the mixture (μM), and its individual components of the mixture corresponding to the highest mixture dose (6.80 μM; EC10). Exposures were repeated at least two times and represents 40–250 individual embryos per exposure group, in total. C) Number of live macrophages per 25 embryos upon exposure to a dose-range of the mixture and selected individual components corresponding to the highest mixture dose (6.80 μM; EC10). Pvalues were calculated using Kruskal Wallis with Dunn's correction for multiple comparisons for the neutrophil density and using a two-sided *t*-test for the live macrophage count, comparing respective exposure group with the DMSO control. In both cases, statistical significance is denoted with asterisks; *0.05, **0.01, ****0.0001, or no significance (ns).

cholesterol biosynthesis, lipid and amino acid metabolism, cell death, inflammatory response and oxidative stress (Förlin, 2019; Kanerva et al., 2020). Altogether, this highlights the need for an improved mechanistic understanding of how exposure to chemical mixtures and mixture components may feed into the observed severe health effects in wild fish in the Baltic Sea for future risk assessment and risk management applications.

Our zebrafish embryo transcriptome results depict a clear temporal dynamic of dose-responses along development. The highest number of DEGs and affected biological functions were identified at 5dpf for dose 2, followed by dose 1 at the same time point. The numbers of DEGs at 3dpf were around six and four-times lower for dose 1 and dose 2 in comparison with corresponding doses at 5dpf. This observation correlates with increasing internal concentrations of DDE, PCB118, PCP,

PFOS and PFOA in zebrafish embryo over time, but is inversely related to the internal concentrations of 4-OH-6CB187, 6-OH-BDE47, 2'-OH-BDE68 and 6-OH-BDE90 (Table 1, (Lindqvist and Wincent, 2022) with decreasing concentrations observed already between 1- and 3dpf. More thorough time-kinetics would thus be needed to distinguish between direct and indirect effects of the mixture as compared to the separate components.

Overall, the molecular and cellular functions most highly affected included drug metabolism, metabolic homeostasis, and immune system function. Drug metabolism was identified to be significantly affected in exposed embryos at 3dpf, reflected by the DEGs clustered in module 2. Here, gene responses of enzymes involved in antioxidant reactions and detoxification such as *prdx1, cyp1a, cyp3a7 and gstp1* were highly similar between the mixture and 6-OH-BDE90 indicating 6-OH-BDE90 to be an important driver of this effect (Fig. 5). These results align with previous findings that collectively demonstrated elevated EROD activity (reflecting CYP1A function) in wild fish and zebrafish exposed to mixtures of chemical stressors from the Baltic Sea (Dahlgren, et al., 2022; Förlin, 2019; Halden, 2011; Dabrowska et al., 2014), and a positive correlation between 6-OH-BDE90 concentration in flounders from the southern Baltic Sea and hepatic EROD activity (Dahlgren, et al., 2022).

All major OH-PBDEs detected in Baltic Sea biota have been observed to impair oxidative phosphorylation (OXPHOS). Among these, 6-OH-BDE47 has shown to be the most potent and to cause synergistic effects on OXPHOS when dosed together with other OH-PBDEs (Legradi, 2014; Legradi et al., 2017). Other halogenated phenolic compounds (HPCs) also disrupt OXPHOS. Considering that more than a hundred different HPCs have been detected in blood from Baltic Sea salmon, including OH-PBDEs (Asplund et al., 1999), this group of compounds are likely major drivers of impaired metabolic function together with PFAS that have also been observed to be potent disruptors of OXPHOS (Starkov and Wallace, 2002). In our study, several genes related to metabolic function were identified as differentially expressed at both 3dpf (modules 2–3) and 5dpf (modules 5–6), including genes associated with metabolism of lipids, fatty acids, steroids, vitamins and minerals, amino acids, and carbohydrates, in addition to energy production. Altogether, these effects suggest that the mixture has a much wider effect on metabolic homeostasis than impaired OXPHOS. Looking at the results from exposure to individual mixture components, DEGs clustered in modules 3 and 5 showed a relatively homogenous effect of all compounds, while PFOS was the only compound correlating with the mixture in module 6, including effects on *angptl3, elovl2* and *soat1*, genes involved in regulation of fatty acid elongation and lipid metabolism (Fig. 5).

Strictly regulated interactions between metabolic functions and the immune system are evolutionarily conserved and critical for tissue function and organismal health. However, the precise mechanism of their reciprocal interaction, in which cellular and systemic metabolism affect immune function and vice versa is less understood (Gleeson and Sheedy, 2016). For example, enhancement of glycolytic pathway is necessary for the downstream function such as inflammatory cytokine and nitric oxide production in macrophages, and the status of OXPHOS in macrophages strongly affects the inflammatory responses. It is also well known that diseases related to impaired metabolic homeostasis such as diabetes, obesity and atherosclerosis are associated with chronic dysregulation of innate immune cells, with a potential adverse effect on the response to pathogens (Gleeson and Sheedy, 2016; Hotamisligil, 2017). Considering the significant effects on metabolic pathways observed with our mixture, this indicates a plausible mechanistic link to impaired immune system development and function. Indeed, suppression of immune system function was one of the most striking outcomes of all functional annotations derived in this study. Such effects were observed already at 3dpf, including chemotaxis of neutrophils, reduced leukocyte migration and reduced inflammation. At 5dpf, suppression of immune functions was clearly increased by the number of functions annotated, the degree they were affected, and their statistical significance, as displayed in gene module 4 (Fig. 4). This was mainly observed as suppression of development, differentiation, and migration of leukocytes, specifically cytotoxic CD8 + T lymphocytes and myeloid cells. Leukocyte infiltration and their functional differentiation are fundamental multistep processes to respond to external stimuli at sites of infected, injured, or stressed tissue (Nourshargh and Alon, 2014), processes that are also dependent on metabolic function (Marelli-Berg and Jangani, 2018).

In line with our findings of suppressed immune functions, others have previously shown that reduced counts of leukocytes were significantly associated with higher body concentrations of 2,4,6-tribromophenol (TBP), 6-OH-BDE47 and the sum of OH-PBDEs and bromophenols in female European flounders caught in Hanöbukten in August 2018 (Dahlgren, et al., 2022). Förlin *et al.* (Förlin, 2019) also identified a significant decrease in number of leukocytes associated with an enriched inflammatory response in female perch collected from Kvädöfjärden in 2014 compared to those collected in 2010. Although Kvädöfjärden is a reference site without any known point source of pollution, increased levels of brominated indoles and methylindoles naturally produced by algae were detected (Förlin, 2019). Moreover, an increased occurrence of the red skin disease has been observed in Atlantic salmons and other wild fish species over the last decade, presumably caused by pathogen infections (Weichert, 2021; SVA, 2017). Chemically caused suppression of immune functions might therefore be a critical key event underlying the drastic increase in infection-related diseases, with potentially long-lasting ecological consequences in wild fish populations.

Chemical effect drivers in Baltic Sea mixture exposures associated with impaired immunity have not yet been identified. While limited knowledge on immunotoxicity of the anthropogenic chemicals PCP and DDE exists, the immunotoxicity of PFOS across different species, including humans, is well documented (DeWitt et al., 2012; DeWitt JC). Immune-related effects of PFOS in fish have been reported for freshwater tilapia (Han et al., 2012) and marine medaka (Huang, 2015), as well as in amphipods (Jacobson), altogether, suggesting a potential association with observed health effects in Baltic Sea salmon. In this study, a partial overlap between immune-related effects induced by individual exposures and the mixture was observed with most compounds, depending on the dose. Of the compounds tested, the low dose of 6-OH-BDE90 (dose 1) elicited the highest similarity with the mixture, suggesting that 6-OH-BDE90 may be an important driver of the observed suppression of immune functions. A partial overlap, including the genes *mx, cmpk2*, *dram1, stat4*, and *gbp1*, was seen at exposure to PFOS, DDE, and 6-OH-BDE47, depending on dose, while PCP showed an almost completely opposite gene response compared to the mixture (Fig. 5). This is in agreement with some of the reported findings on immune status from ecoepidemiology studies (Dahlgren, et al., 2022; Förlin, 2019), though the mechanisms on how 6-OH-BDE90 modulates immunological functions have, to the best of our knowledge, not yet been described.

The results on suppressed immune functions were strongly supported by the tissue injury model, in which a dose-dependent suppression of innate immune cell translocation to the damage was observed at exposure to the mixture, as well as to some of the individual components (Fig. 6). The significant reduction of total macrophages further corroborated the immune suppressive potential, altogether confirming effects at both the level of immune development and function. As suggested from the transcriptional effects, the two main OXPHOS inhibitors in the mixture, 6-OH-BDE47 and 6-OH-BDE90, showed the strongest association with immune suppression. While both generated a strong suppression of neutrophils recruitment, 6-OH-BDE47 was the obvious driver of the reduced number of macrophages. These results are of particular concern for species in the Baltic Sea whose fry grow up in the shallow littoral zone and associated wetlands, as the production of 6-OH-BDE47 by filamentous macroalgae can become very high in these areas during the summer (Dahlgren et al., 2016).

The knowledge of chemical pollution and toxic body burden at Baltic

Sea reference sites is currently fragmented. Our findings strongly suggest that exposure to natural and anthropogenic halogenated toxins may severely hamper the health of fish, particularly their resistance to and recovery from various infections and injuries, effects that have been clearly demonstrated in different studies of Baltic Sea wildlife health (Weichert, 2021; Brockmark, 2017; Brockmark, 2019; SVA, 2017; Dahlgren, et al., 2022; Sonne, 2020; Förlin, 2019). Our results also indicate that while different components of the mixture are clear drivers of immune suppression, the total mixture may be required for the wider effects on immune function. Performing additional studies with fish models testing e.g. the ability to fight bacterial or fungal infections would increase the insight on width of potential consequences of the observed immune suppression, and their underlying mechanisms of action.

While our study bring forth novel and important data on the toxicity of chemicals found in the Baltic Sea, some limitations are important to underline, such as the use of a fish species not native to the Baltic Sea as experimental model, and including only a subset of the many chemicals found in this environment. To address these limitations going forward, the transcriptional profiling performed in this study could be used to pinpoint molecular effect markers to analyse in wild fish from the Baltic Sea alongside chemcial profiling of different tissues and serum, to delineate the environmental impact on the health of Baltic Sea wild fish. In summary, this is the first study investigating the toxicity mechanisms of an environmentally relevant mixture composed of several chemical classes originating from anthropogenetic and natural sources found in the Baltic Sea. Minimizing the potential toxicokinetic differences between zebrafish and Baltic Sea salmon enabled us to determine transcriptional and functional effects of the same relative internal doses of mixture components as detected in the salmon serum. Using a data-driven approach, we furthermore studied toxicity mechanisms to identify the effect drivers of one or multiple compounds in the mixture. We developed a bioinformatics pipeline to analyze perturbed molecular and cellular functions, identify drivers of gene responses, and validate critical effects functionally. All together, this study significantly advances our understanding of the mechanisms and health impacts of chemical pollutants on wild fish in the Baltic Sea. Since these environmental toxins also affect other wildlife and humans, our results highlight their broader relevance to chemically induced health effects.

Disclosure

We declare that this manuscript is original, has not been published before and is not currently being considered for publication elsewhere. We confirm that the manuscript has been read and approved by all named authors and that there are no other persons who satisfied the criteria for authorship but are not listed. We further confirm that the order of authors listed in the manuscript has been approved by all of us. We understand that the Corresponding Author is the sole contact for the Editorial process. He/she is responsible for communicating with the other authors about progress, submissions of revisions and final approval of proofs.

CRediT authorship contribution statement

Carolina Vogs: Writing – review & editing, Writing – original draft, Visualization, Formal analysis, Data curation. **Dennis Lindqvist:** Writing – review & editing, Writing – original draft, Methodology, Funding acquisition, Formal analysis, Conceptualization. **Sheung Wai Tang:** Methodology, Investigation, Formal analysis. **Lydia Gugescu:** Methodology, Investigation, Formal analysis, Data curation. **Harri Alenius:** Writing – review & editing, Writing – original draft, Visualization, Formal analysis, Data curation. **Emma Wincent:** Writing – review & editing, Writing – original draft, Visualization, Funding acquisition, Formal analysis, Data curation, Conceptualization.

Declaration of competing interest

The authors declare that they have no known competing financial interests or personal relationships that could have appeared to influence the work reported in this paper.

Data availability

Data will be made available on request.

Acknowledgement and funding sources

This work was funded by FORMAS a Swedish council for sustainable development [grant numbers 2018-01571 and 2021-00711]. Disclosure: The authors declare no competing financial interest.

Appendix A. Supplementary data

Supplementary data to this article can be found online at https://doi.org/10.1016/j.envint.2024.109018.

References

Airaksinen, R., et al., 2014. Time trends and congener profiles of PCDD/Fs, PCBs, and PBDEs in Baltic herring off the coast of Finland during 1978–2009. Chemosphere 114, 165–171.

Asplund, L.T., Athanasiadou, M., Sjödin, A., Bergman, Å., Börjesson, H., 1999. Organohalogen substances in muscle, egg and blood from healthy Baltic salmon *(Salmon salar)* and Baltic salmon that produced offspring with the M74 syndrome. Ambio 28 (1), 67–76.

Bergman, A., 1999. Health condition of the Baltic grey seal (Halichoerus grypus) during two decades - Gynaecological health improvement but increased prevalence of colonic ulcers (vol 107, pg 270, 1999). APMIS : Acta Pathologica, Microbiologica, et Immunologica Scandinavica 107 (9), 886.

Bignert, A., Danielsson, S., Faxneld, S., Nyberg, E., 2016. Comments Concerning the National Swedish Contaminant Monitoring Programme in Marine Biota. Swedish Museum of Natural History, Stockholm, Sweden.

Bjurlid, F., Roos, A., Jogsten, I.E., Hagberg, J., 2018. Temporal trends of PBDD/Fs, PCDD/Fs, PBDEs and PCBs in ringed seals from the Baltic Sea (Pusa hispida botnica) between 1974 and 2015. Sci. Total Environ. 616, 1374–1383.

Bonsdorff, E., Rönnberg, C., Aarnio, K., 2002. Some ecological properties in relation to eutrophication in the Baltic Sea. Hydrobiol 475 (476), 371–377.

Brockmark SC, H., 2017. Sjuklighet och dödlighet i svenska laxälvar under 2014–2016. (Swedish national veterinary institute (SVA)), pp 1-58.

Brockmark, S.C., H. 2019. Fortsatta undersökningar av laxsjuklighet under 2018. (Swedish national veterinary institute (SVA)), pp 1-43.

Dabrowska, H., Kopko, O., Góra, A., Waszak, I., Walkusz-Miotk, J., 2014. DNA damage, EROD activity, condition indices, and their linkages with contaminants in female flounder (Platichthys flesus) from the southern Baltic Sea. Sci Total Environ 496, 488–498.

Dahlgren, E., Enhus, C., Lindqvist, D., Eklund, B., Asplund, L., 2015. Induced production of brominated aromatic compounds in the alga Ceramium tenuicorne. Environ. Sci. Pollut. Res. Int. 22 (22), 18107–18114.

Dahlgren, E., Lindqvist, D., Dahlgren, H., Asplund, L., Lehtila, K., 2016. Trophic transfer of naturally produced brominated aromatic compounds in a Baltic Sea food chain. Chemosphere 144, 1597–1604.

Dahlgren, E., et al., 2022. A screening study of relationships among concentrations of algal toxins, PFAS, thiamine deficiency and biomarkers in the European flounder from the southern Baltic Sea. Reg Stud Mar Sci 53.

d'Alencon, C.A., et al., 2010. A high-throughput chemically induced inflammation assay in zebrafish. BMC Biol. 8, 151.

de Wit, C.A., et al., 2020. Organohalogen compounds of emerging concern in Baltic Sea biota: Levels, biomagnification potential and comparisons with legacy contaminants. Environ. Int. 144, 106037.

DeWitt, J.C., Blossom, S.J., & Schaider, L.A. (Exposure to per-fluoroalkyl and polyfluoroalkyl substances leads to immunotoxicity: epidemiological and toxicological evidence. (1559-064X (Electronic)).

DeWitt, J.C., Peden-Adams, M.M., Keller, J.M., Germolec, D.R., 2012. Immunotoxicity of Perfluorinated Compounds: Recent Developments. Toxicol. Pathol. 40 (2), 300–311.

Faxneld, S., et al., 2016. Temporal trends and geographical differences of perfluoroalkyl acids in baltic sea herring and white-tailed sea eagle eggs in Sweden. Environ. Sci. Tech. 50 (23), 13070–13079.

Faxneld, S., Nyberg, E., Danielsson, S., & Bignert, A., 2014. Miljögifter i biota. in *Havet* (Havet), pp 78-81.

Förlin, L., et al., 2019. mRNA Expression and Biomarker Responses in Perch at a Biomonitoring Site in the Baltic Sea – Possible Influence of Natural Brominated Chemicals. Frontiers in Marine Science 6.

Gleeson, L.E., Sheedy, F.J., 2016. Metabolic reprogramming & inflammation: Fuelling the host response to pathogens. Semin Immunol 28 (5), 450–468.

Gustafsson, J., et al., 2021. Correlating seasonal changes of naturally produced brominated compounds to biomarkers in perch from the Baltic Sea. Aquat. Toxicol. 240, 105984.
Halden, A.N., et al., 2011. Retention and maternal transfer of brominated dioxins in zebrafish (Danio rerio) and effects on reproduction, aryl hydrocarbon receptor-regulated genes, and ethoxyresorufin-O-deethylase (EROD) activity. Aquat. Toxicol. 102 (3–4), 150–161.
Han, Z., Liu, Y., Wu, D., Zhu, Z., Lü, C., 2012. Immunotoxicity and hepatotoxicity of PFOS and PFOA in tilapia (Oreochromis niloticus). Chin. J. Geochem. 31 (4), 424–430.
Helcom, 2009. Eutrophication in the Baltic Sea - An integrated thematic assessment of the effects of nutrient enrichment in the Baltic Sea region. In *Baltic Sea Environment Proceedings*.
Hotamisligil, G.S., 2017. Foundations of Immunometabolism and Implications for Metabolic Health and Disease. Immunity 47 (3), 406–420.
Huang, Q., et al., 2015. Immunotoxic effects of perfluorooctane sulfonate and di(2-ethylhexyl) phthalate on the marine fish Oryzias melastigma. Fish Shellfish Immunol 44 (1), 302–306.
Jacobson, T., et al., (Perfluorooctane sulfonate accumulation and parasite infestation in a field population of the amphipod Monoporeia affinis after microcosm exposure. (1879-1514 (Electronic)).
Kammann, U., et al., 2004. Genotoxic and teratogenic potential of marine sediment extracts investigated with comet assay and zebrafish test. Environ. Pollut. 132 (2), 279–287.
Kanerva, M., Tue, N.M., Kunisue, T., Vuori, K., Iwata, H., 2020. Effects on the Liver Transcriptome in Baltic Salmon: Contributions of Contamination with Organohalogen Compounds and Origin of Salmon. Environ. Sci. Tech. 54 (23), 15246–15256.
Legradi, J., et al., 2014. Disruption of oxidative phosphorylation (OXPHOS) by hydroxylated polybrominated diphenyl ethers (OH-PBDEs) present in the marine environment. Environ. Sci. Tech. 48 (24), 14703–14711.
Legradi, J., Pomeren, M.V., Dahlberg, A.K., Legler, J., 2017. Effects of Hydroxylated Polybrominated Diphenyl Ethers in Developing Zebrafish Are Indicative of Disruption of Oxidative Phosphorylation. Int. J. Mol. Sci. 18 (5).
Lindqvist, D., 2020. Screening of halogenated phenolic compounds in plasma and serum from marine wildlife. Int J Environ Sci Te 17 (4), 2177–2184.
Lindqvist, D., Wincent, E., 2022. Kinetics and toxicity of an environmentally relevant mixture of halogenated organic compounds in zebrafish embryo. Aquat. Toxicol. 252, 106311.
Lindqvist, D., Dahlgren, E., Asplund, L., 2017. Biosynthesis of hydroxylated polybrominated diphenyl ethers and the correlation with photosynthetic pigments in the red alga Ceramium tenuicorne. Phytochemistry 133, 51–58.
Löfstrand, K., 2011. Trends and exposure of naturally produced brominated substances in Baltic biota -with focus on OH-PBDEs, MeO-PBDEs and PBDDs. PhD (Department of materials and environmental chemistry, Stockholm University, Stockholm, Sweden).
Malmvärn, A., Zebühr, Y., Kautsky, L., Bergman, A., Asplund, L., 2008. Hydroxylated and methoxylated polybrominated diphenyl ethers and polybrominated dibenzo-*p*-dioxins in red alga and cyanobacteria living in the Baltic Sea. Chemosphere 72 (6), 910–916.
Marelli-Berg, F.M., Jangani, M., 2018. Metabolic regulation of leukocyte motility and migration. J. Leukoc. Biol. 104 (2), 285–293.
Marwah, V.S., et al., 2018. INfORM: Inference of NetwOrk Response Modules. Bioinformatics 34 (12), 2136–2138.
Miller, A., et al., 2014. Comparing temporal trends of organochlorines in guillemot eggs and Baltic herring: advantages and disadvantage for selecting sentinel species for environmental monitoring. Mar Environ Res 100, 38–47.
Nourshargh, S., Alon, R., 2014. Leukocyte migration into inflamed tissues. Immunity 41 (5), 694–707.
Nyman, M., Koistinen, J., Fant, M.L., Vartiainen, T., Helle, E., 2002. Current levels of DDT, PCB and trace elements in the Baltic ringed seals (Phoca hispida baltica) and grey seals (Halichoerus grypus). Environ. Pollut. 119 (3), 399–412.
Scala, G., Serra, A., Marwah, V.S., Saarimaki, L.A., Greco, D., 2019. FunMappOne: a tool to hierarchically organize and visually navigate functional gene annotations in multiple experiments. BMC Bioinf. 20 (1), 79.
Sonne, C., et al., 2020. Health effects from contaminant exposure in Baltic Sea birds and marine mammals: A review. Environ Int 139, 105725.
Starkov, A.A., Wallace, K.B., 2002. Structural determinants of fluorochemical-induced mitochondrial dysfunction. Toxicol. Sci. 66 (2), 244–252.
SVA, 2017. Sjuklighet och dödlighet i svenska laxälvar under 2014–2016: Slutrapport avseende utredning genomförd 2016 pp 1-58.
Tal, T., Vogs, C., 2021. Invited Perspective: PFAS Bioconcentration and Biotransformation in Early Life Stage Zebrafish and Its Implications for Human Health Protection. Environ. Health Perspect. 129 (7), 71304.
Tyanova, S., et al., 2016. The Perseus computational platform for comprehensive analysis of (prote)omics data. Nat Methods 13 (9), 731–740.
Weichert, F.G., et al., 2021. A multi-biomarker study on Atlantic salmon (Salmo salar L.) affected by the emerging Red Skin Disease in the Baltic Sea. J. Fish. Dis. 44 (4), 429–440.